Properties of Ultra-High-Molecular-Weight Polyethylene with a Structure Modified by Plastic Deformation and Electron-Beam Irradiation

Jerzy Cybo,[1] Joanna Maszybrocka,[1] Piotr Duda,[1] Zbigniew Bartczak,[2] Adrian Barylski,[1] Sławomir Kaptacz[1]

[1]Department of Materials Science, University of Silesia, Sniezna 2, Sosnowiec 41-200, Poland
[2]Centre of Molecular and Macromolecular Studies, Polish Academy of Sciences, Sienkiewicza 112, Lodz 90-363, Poland

ABSTRACT: To improve the functional properties of polyethylene in a polymer–metal kinematic system, ultra-high-molecular-weight polyethylene (UHMWPE) was subjected to light deformation by uniaxial compression [permanent true strain (e_f) = 0.14–0.32] and postdeformation electron-beam irradiation (with a dose of 26–52 kGy). X-ray examinations demonstrated that no significant reorientation of the lamellar structure occurred upon compression. The textures of all of the samples, except for the sample deformed at e_f = 0.32, were nearly random. In the exception, a very weak axial texture developed. However, the treatment applied (deformation and electron-beam irradiation) significantly changed the structure of the material. A considerable increase in the crosslinked fraction and the crystalline band absorption in the Fourier transform infrared spectra were observed in the modified samples. This indicated a noticeable increase in the degree of spatial ordering within a structure, although the overall crystallinity increased only slightly. The effect of such restructuring was evidenced by microscopic observations of the near-surface layer of the UHMWPE samples subjected to unidirectional sliding interaction with a CoCr alloy for 100 h (in a block-ring tribological system). It was found that for the predeformed (e_f = 0.14–0.21) and electron-irradiated (dose of 52 kGy) samples, the operational load imposed on the system resulted in a considerable reduction in the thickness of the plastically deformed near-surface layer and in a decreasing amount of lamellae oriented flat-on compared to the neat unmodified UHMWPE subjected to the same test. The recorded tribological wear (mass decrement) decreased up to fivefold in comparison to that of the initial material. © 2012 Wiley Periodicals, Inc. J Appl Polym Sci 000: 000–000, 2012

Key words: irradiation; mechanical properties; plastics

INTRODUCTION

There is a high demand for significant improvements in the operational durability of kinematic systems of the polymer–metal type. This refers to both engineering and biomedical applications (e.g., endoprostheses of knee and hip joints). From the point of view of resilience to impact and fatigue loads and the susceptibility for cracking and brittle fracture, higher elastic and plastic compliance of a polymer at the macroscopic (structural) scale are highly desired. The ultra-high-molecular-weight polyethylene (UHMWPE) is frequently used as a material for slide bearings or polymer–metal joints. Despite the numerous advantages of this material, its main deficiency is a serious transformation of an upper layer during the operation of the polymer–metal kinematical system due to its susceptibility to plastic deformation and wear

(abrasive and through adhesive tacking). The problem is particularly severe because the excessive wear of the polyethylene (PE) part of an artificial joint and the resulting formation of particulate debris from the articulating surface leads to the reaction of the wear products with surrounding tissues. This may cause osteolysis and, consequently, a loosening of the implant; this, in turn, leads to a need for reimplantation of the artificial joint in the human body.[1–3]

There have been many attempts to enhance the functional properties of PE, including the modification of its structure through deformation and/or crosslinking by irradiation (e.g., refs. [4] and [5]). It is recommended that the optimization of polymer resistance to wear and aging be based on the idea of ensuring a high molecular weight, appropriate proportion of high- and low-molecular fractions, and a balanced crystalline-to-amorphous phase ratio.[4] A significant role in the modification of properties of a polymer for joint replacement is also played by the irradiation of the material with γ radiation or, more and more frequently, an electron beam. Doses higher than 25 kGy lead to fragmentation of long chains, some spatial rearrangement of the structure, and at the same time,

crosslinking. A larger dose of electrons (even up to 150 kGy) combined with postirradiation thermal treatment causes the stabilization of free radicals and increased resistance to oxidation and, most important, results in a very significant reduction of wear. The wear of UHMWPE observed in simulators could be reduced to merely 20 mg per million cycles.[6–9]

An analysis of the literature shows that, in general, two trends leading to increased resistance of polymers to wear can be distinguished: a modification of the chemical structure (e.g., by various chemical reactions, ion implementation, or chemical or irradiation crosslinking) and an alteration of the physical microstructure (e.g., through thermal, thermomechanical, or high-pressure treatment). There are also many combinations of those methods described in the literature. Crosslinking through irradiation, for example, with γ radiation, can precede the deformation and texturing processes (which can then be performed at higher temperatures of 110–200°C)[10–12] or can be applied after deformation of the material.[12] In the majority of methods applied to alter the PE structure and properties, posttreatment annealing is additionally used to stabilize the structure. It reduces the residual stresses and anisotropy of properties and chemically stabilizes PE (in terms of oxidation resistance) by the recombination of a significant fraction of free radicals.[10–13] However, such a posttreatment annealing is sometimes omitted.[14]

In the case of a modified material demonstrating a preferred orientation and anisotropic properties, the location of the sample, especially the orientation of the working surface of the acetabular cup of the endoprosthesis with respect to the direction of that orientation, is of utmost importance. An increase in the resistance to wear by 3–5 times is frequently observed in such systems but only when the plane of the tribological interaction is parallel to the direction of the prior deformation, whereas the direction of movement/sliding is preferentially perpendicular to that deformation direction.[11–14] Marrs et al.[12] suggested, however, that such a significant improvement in the tribological properties can be achieved only in the case of a bidirectional or multidirectional movement during the interaction with a smooth surface of the CoCr counterspecimen. When the surface of the material is rough or the movement is unidirectional, the material modified by deformation or γ irradiation demonstrates much less reduction in wear or even, for a unidirectional movement, the wear increases by as much as 1.4–2 times compared to that of the nonmodified raw material (UHMWPE of the GUR 1120 grade).[12]

The methods of modification of UHMWPE for the implants outlined previously are relatively complicated, labor-consuming, and costly, and the final outcome depends on the UHMWPE working surface location, type of movement (unidirectional vs multidirectional), and surface roughness of the metallic counterpartner. Therefore, it would be highly desirable to develop a method of modification of the UHMWPE biopolymer that would be cheaper, easy to apply, and effective as far as the improvement of the resistance of the UHMWPE upper layer to wear and plastic deformation is concerned. Our concept of such a method relied on a light plastic deformation of PE (e.g., by cold compression to a strain of 0.1–0.3) to initiate a process of fine morphological adjustment, during which the crystalline phase would started to orient yet did not undergo heavy reorientation, whereas the lamellar microstructure preserved the global isotropy of the initial material. The synergic enhancement of the morphological changes in the polymer was expected to be achieved by postdeformation irradiation with an electron beam (the use of electron-beam irradiation is cheaper, faster, and safer than that of γ irradiation). As a result of these two treatments, an improvement in the mechanical and wear properties was expected because of the modified and stabilized structure and morphology. It was decided that PE modified according to such a method, with a nearly random lamellar microstructure and quasi-isotropic properties, would not be subjected to thermal stabilization at this stage of the research. The material was only aged (seasoned) at room temperature for 6 months.

We chose to examine the mechanical and tribological properties of the modified UHMWPE under the following conditions:

- The surface of tribological interaction was parallel to the deformation direction, and the movement (sliding) direction was perpendicular to it.
- Taking advantage of an assumed quasi-isotropy of the lamellar microstructure of the modified material, we placed the surfaces of the samples used for micromechanical and sclerometric tests perpendicular to the deformation direction, but the scratching direction during scratch testing was perpendicular to the compression direction.

Some early results of the preliminary stages of the examination of UHMWPE modified with this method were published earlier.[15–19] The aim of this work was to document the performance of a combined action of the plastic deformation and radiation crosslinking processes for a significant reduction of wear and susceptibility of UHMWPE to permanent deformation due to kinematical friction.

EXPERIMENTAL

Material and sample preparation

The neat input material (code BZ) for this study was a rod of UHMWPE Chirulen 1120, (Quadrant PHS

TABLE I
UHMWPE Samples Used in This Study

| UHMWPE GUR 1120 | e_f | Electron irradiation dose | | |
		0	1×26 kGy	2×26 kGy
Height	0	0	BZ	1	2
reduction (%)	15	0.14	A	A1	A2
	30	0.21	B	B1	B2
	45	0.32	C	C1	C2

BZ, initial material; 1 and 2, BZ materials after irradiation with one and two doses, respectively. The A1, B1, C1, A2, B2, and C2 samples were irradiated once and twice after initial deformation.

Deutschland GmbH, Vreden, Germany), manufactured by the compression molding of medical-grade UHMWPE powder (GUR 1120, Ticona GmbH, molecular weight $\approx 5 \times 10^6$, density $= 0.93$ g/cm^3). This material has been used widely until recently as a semifinished product for endoprosthesis acetabular cups.

The structure of this PE was modified in two steps: (1) low-strain plastic deformation followed by (2) electron-beam irradiation. In the first step, cylindrical sections of the Chirulen rod (60 mm in diameter and 12 mm high) were deformed by uniaxial compression to obtain compression degrees of $Z = 15$, 30, and 45% [in terms of thickness reduction, $Z = (H_0 - H')/H_0 \times 100\%$, where H_0 is the height of the sample before deformation and H' is the height of the compressed sample still under load]. The compression was conducted on a WEB ZD40 press (VEB WerksoffMaschinen, Leipzig, Germany) (maximum pressure $= 400$ kN) with a crosshead speed of 5 mm/min at room temperature. After the desired thickness was reached, the sample was immediately unloaded. Next, the sample was left for strain recovery for several days at room temperature, and the permanent true strain (e_f; the Hencky strain) was determined: $e_f = \ln(H_0/H_f) = 0.14$, 0.21, and 0.32 (where H_f is the final sample height after recovery, measured 10 days after the compression experiment). The values of e_f not exceeding 0.32 indicate that all of the samples were deformed far below the strain-hardening region ($e_f \geq 1$), where a significant orientation of the crystalline phase occurred.[20–22]

In the second step of the treatment, the deformed and fully recovered UHMWPE samples were irradiated with an electron beam with a linear electron accelerator (Institute of Nuclear Technology, Warsaw, Poland), with the application of a 10-MeV energy beam. The dose delivered to the sample in a single pass was 26 kGy. The samples were irradiated in one or two passes, so the total dose was either 26 or 52 kGy. Table I summarizes the samples prepared and investigated in this study.

The samples obtained by modification according to our procedure were not stabilized thermally by

the postannealing because the process parameters were not yet optimized. The material was only seasoned for 6 months at room temperature, with the samples being kept in a PE bag in an exsiccator. The location and orientation of specimens cut from the compressed and irradiated samples and intended for further studies are depicted in Figure 1. The circumference region of the compressed material was not used, as it could have contained some unwanted cracks or fissures.

Characterization

To determine the changes in the structure of the polymers after the applied procedures, the following tests were conducted:

- The content of the insoluble (high-molecular) fraction (*hmf*) was estimated by extraction with trichlorobenzene at a temperature of 150°C for 66 h.
- Differential scanning calorimetry (DSC): Thermal analysis was conducted with a TA 2100 DSC apparatus (TA Instruments, New Castle,
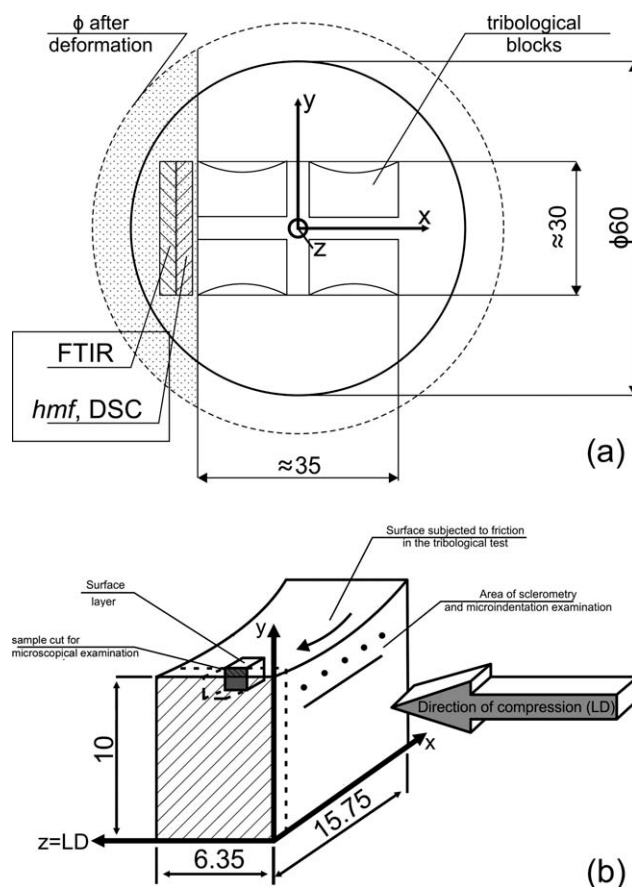

Figure 1 (a) Illustration of the compressed sample and the location of specimens machined out for the tribological and structural studies. The LD was perpendicular to the figure plane. (b) Details of the specimen used for the tribological and micromechanical studies.

DE, USA). The melting thermograms were recorded at a heating rate of $10°/min$ under a nitrogen flow. The crystallinity was estimated on the basis of the heat of melting of the sample, with the assumption that the heat of melting of 100% crystalline PE was 293 J/g.[23]

• Fourier transform infrared (FTIR) spectroscopy: The FTIR spectra were collected with an ATI Mattson Infinity FTIR 60 infrared spectrometer (Mattson Instruments, Inc., Madison, WI, USA) (32 scans, resolution = 2 cm^{-1}) at several locations for each specimen. The averaging, corrections, and normalization of the spectra were performed according to the procedure described in ref. [24]. The analytical differential spectra were obtained by subtraction of the corrected spectrum of the raw PE (BZ sample) used as a reference from the corrected spectra of the modified samples. For analysis of the crystal phase, the changes in the absorbance of the so-called crystallinity band at 1898 cm^{-1}, assigned to combination modes of crystalline vibrations, was analyzed. This band refers to the number of chains oriented in a parallel fashion; due to chain folding, this enables the molecule to form crystalline lamellae.[25] Therefore, the changes in the absorbance of this band with respect to the initial polymer can be used as a measure of the evolution of spatial ordering of the modified sample [degree of spatial arrangement (sa)].

• Scanning electron microscopy: The specimens for microscopic observations were prepared by permanganic etching (ca. 1 h at room temperature) with a mixture containing 0.7 w/v $KMnO_4$ dissolved in a 5 : 4 : 1 v/v mixture of 95% sulfuric acid, 85% phosphoric acid, and distilled water, respectively, according to the procedure developed originally by Olley et al.[26] The etched, washed, and dried specimens were coated with a fine gold layer by ion sputtering (JEOL JFC-1200) and examined with a scanning electron microscope (JEOL JSM-5500LV, Tokyo, Japan) operating in the high vacuum mode at an accelerating voltage of 10 kV.

X-ray examination of the PE structure and orientation

The orientation of the lamellar and crystalline structures were probed by two-dimensional small-angle X-ray scattering (2-D SAXS) and wide-angle X-ray scattering (pole figures), respectively.

The lamellar structure was examined by 2-D SAXS. The 1.1 m long Kiessig-type camera was equipped with a tapered capillary collimator (XOS) combined with additional pinholes (300 µm in diameter) form-

ing the beam, and an imaging plate as a detector (Fuji). The camera was coupled to a X-ray source (sealed-tube, fine-point Cu Kα filtered radiation operating at 50 kV and 40 mA; Philips Medizin Systeme GmbH, Hamburg, Germany). Specimens for SAXS examination were cut along the loading direction (LD) so that the plane normal to the specimen was parallel to the transverse direction (and coincided with the radius of the deformed sample). The time of collection of the pattern was usually 3 h. The exposed imaging plates were read with a Phosphor Imager SI scanner and ImageQuant software (Molecular Dynamics).

The crystalline texture of the deformed samples was studied with the X-ray pole figure technique. A wide-angle X-ray scattering system consisted of a computer-controlled pole figure attachment associated with a goniometer (DRON, Bourevestnik, Inc., St. Petersburg, Russia) coupled with a sealed-tube source of filtered Cu Kα radiation operating at 30 kV and 30 mA (Philips). The specimens, in the form of 1 × 1 cm^2 slices and approximately 1 mm thick, were cut out of the deformed samples in the plane perpendicular to the LD. Such an orientation of specimens allowed us to reduce the influence of analytical errors resulting from the defocusing of the beam when the specimen was tilted during data collection. The slits and the pinhole collimator limited the size of the beam and illuminated the sample to maximum 4 × 4 mm^2 for the largest specimen tilt. The following diffraction reflections from the orthorhombic crystal form of PE were analyzed: (110), (200), (020), and (002), positioned at 2θ = 21.6, 24, 36.4, and 74.5°, respectively. The pole figure plots were generated by the POD program, a part of the popLA package (Los Alamos National Laboratory, Los Alamos, New Mexico). The other details of the technique of pole figure preparation were described elsewhere.[27]

Estimation of the mechanical properties by microindentation and sclerometry methods

The micromechanical properties were probed with microindentation and sclerometric tests. The microindentation measurements were conducted with a Micro-Combi tester manufactured by CSM (CSM Instruments SA, Peseux, Switzerland). The microhardness (H) was tested with a Berkovich indenter with a pyramid angle of 65° under 1 N of force, applied at a load rate of 1 N/min. The time under the full load was 5 s. After that period, the sample was unloaded at the same rate. For each measurement, a force/penetration depth curve was recorded. H was determined as the ratio of maximum force to the actual area of indenter contact with the material. The size of the contact area was determined on the bases of the indenter geometry and the size of the indentation trace. The elasticity modulus (E) was
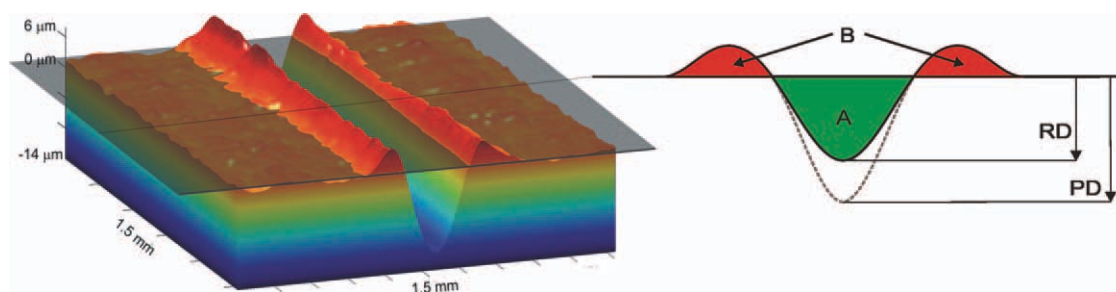
Figure 2 Isometric image and crossection of the scratch line in the sclerometric test. [Color figure can be viewed in the online issue, which is available at wileyonlinelibrary.com.]

calculated from the slope of the unloading curve, approximated with a second-rank polynomial.

Sclerometric tests were performed with a TalySurf profilometer (Taylor Hobson, Leicester, United Kingdom). Controlled scratching of the surface was carried out with a Rockwell penetrator with a blade rounded to 200 nm, with the application of a constant force of 5 N and a shift speed of 9.59 mm/min for a 10 mm long scratch. The penetrator indentation, which can be regarded as the measure of a polymer's susceptibility to scratching, was assessed as the working scratch depth (PD; during a scratch test) and the permanent scratch depth (RD; measured after elastic recovery). On the basis of a stereometric analysis of the scratch traces, the cross-sectional surface area of the plastic elevation of the material (B) and that of the scratch groove (A; see Fig. 2 for explanation of symbols) and the ratios of the abrasive wear micromechanism (β's) were determined with a TalyMap Universal program (Taylor-Hobson Co.):

$$\left(\beta = \frac{1}{n} \sum_{i=1}^{n} \frac{A - B}{A} \right)$$

Tests of the resistance to tribological wear

The specimens of raw and modified UHMWPE, listed in Table I, were subjected to interaction in the kinematic node of a block-cylinder type T-05 tribological tester (IteE, Radom, Poland); this enabled us to maintain the conditions specified in ASTM standards. Figure 3 shows the diagram of the system, where the PE sample (1) mounted in the grip (4) was pushed through a hemispherical spacer (3) to the rotating countersample (2) made of CoCr alloy (Vitalium, Faculty of materials engineering and metallurgy, Silesian University of Technology, Katowice, Poland). The surfaces of the interacting elements were prepared according to ISO 7206-2. The couple used reflects in the first approximation the working conditions of an endoprothesis. In the tested system, the surface of the tribological interaction of the polymer block remained parallel to the direction of the prior-deformation LD, whereas the direction of movement (sliding) was per-pendicular to it (cf. Figs. 1 and 3). Preliminary experiments with the oscillatory motion (f) of the countersample demonstrated very low, difficult to accurately measure mass wear of the PE blocks. Therefore, we decided to conduct the wear test with a unidirectional rotary motion of the countersample (n). The sliding speed was set to 0.25 m/s (rotational speed = 2.5 rps) and a friction distance of 90 km (test time = 100 h). The stress in the friction couple was 7 MPa. The system was lubricated with a Ringer's solution at a temperature of 36 ± 2°C delivered with a peristaltic pump in the amount of 2 mL/min with a closed lubricant circulation (without filtration of the wear products). The ambient conditions were as follows: temperature = 21 ± 1°C and humidity = 50 ± 5%. To avoid distortions in the assessment of wear, the polymer blocks were immersed for 3 days in the Ringer's solution before the experiment. After the tribological test, they were cleaned with distilled water in an ultrasonic bath, dried with tissue paper, and stored in an exsiccator.

RESULT AND DISCUSSION

Crystalline phase texture and lamellar structure orientation

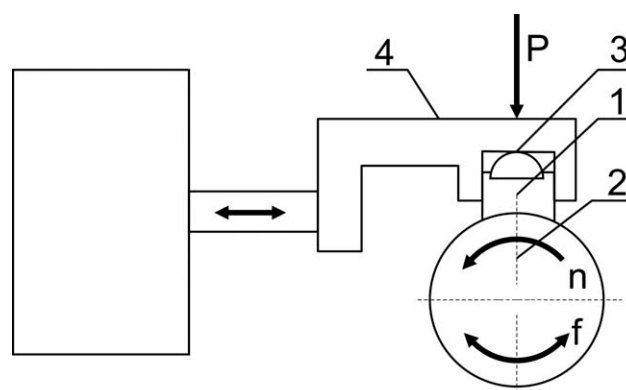An analysis of the diffraction patterns and positions of crystalline peaks showed that practically all

Figure 3 Diagram of the tribological setup: (1) polymer sample, (2) rotating CoCr alloy countersamples, (3) hemispherical spacer, and (4) grip.

crystallites in the raw, deformed as well as deformed and irradiated samples, belonged to an orthorhombic modification, typical for PE. This means that orthorombic crystals present in the initial material were not transformed by other modification, neither deformation nor electron-beam irradiation. The pole figures, which map the orientation of a particular crystallographic plane, were determined for the (110), (200), (020), and (002) planes of the orthorombic system. Figure 4 presents a representative set of pole figures of the (200) plane evaluated for the samples studied. These figures are plotted in stereographic projection along the LD, that is, with the LD normal to the figure-drawing plane. In such a projection, one can expect a completely flat figure for the unoriented sample, whereas for samples of uniaxially compressed PE, the pole figures in the form of a ring centered around LD, typical for an axial (fiber) texture. In the axial texture, crystallites are oriented preferentially with their (200) planes at some angle with respect to the LD; hence, the (200) normals defined a cone, which gave a trace in the form of the ring around the LD in the pole figure. The experimental pole figures of the raw sample BZ confirmed a random crystal orientation; the (200)-pole figure (cf. Fig. 4) and the pole figures of the other measured planes (not shown here) were almost flat, with the intensities fluctuating around 1 multiple of random distribution. For deformed samples, one can observe in (200)-pole figures a faint outline of the ring of higher intensity centered around the LD, as expected for an axial texture. That feature was recognized in samples C–C2 of the highest strain in the series (compressed by 45%, $e_f = 0.32$), whereas for samples A and B of the lower strain ($e_f = 0.14$ and 0.21, respectively), it was barely visible (the broad culmination of intensity in the center of the pole figures was a result of a beam defocusing effect rather than weak orientation). Even for the highest deformation of samples C and C2, the intensity at the maximum ring reached only 1.6 multiples of random distribution; this indicated a rather weak orientation.

The lamellar orientation was probed with 2-D SAXS in samples illuminated with X-rays along the radial direction (perpendicular to the LD). Material of random distribution of lamellar orientation should produce a circular 2-D SAXS pattern, whereas an elliptical distortion of the pattern indicates a preferred orientation of lamellae and changes in the long period related to the orientation of the structure. As shown in Figure 5, all patterns, including that of the raw sample BZ, exhibited a slightly elliptical shape with a long axis of the ellipse oriented along the LD. These patterns indicated a weak orientation of lamellae, present already in the raw, nondeformed sample (which was a rod produced by
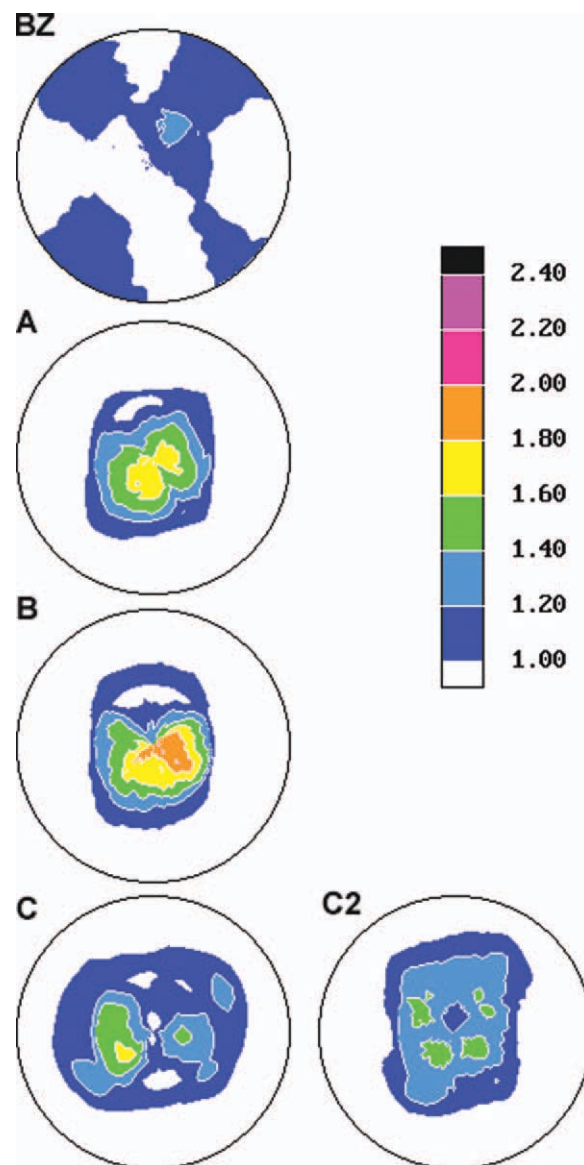

Figure 4 Normalized pole figures of the (200) crystallographic plane of orthorhombic PE determined for the UHMWPE samples: virgin sample (BZ), samples deformed uniaxially (A, B, and C), and sample deformed and irradiated with a dose of 52 kGy (C2). Refer to Table I for the sample codes. The figure parts are plotted in the sterographic projection with a linear scale. The LD is normal to the projection plane. [Color figure can be viewed in the online issue, which is available at wileyonlinelibrary.com.]

extrusion). The direction of the preferred orientation of lamella normals was along the LD. Such a low orientation was apparently a result of structural formation upon solidification of the material during its extrusion (the direction of extrusion coincided with the LD). Comparing the patterns of samples deformed by uniaxial compression with that of the initial sample BZ, we concluded that the plastic deformation in the low range of strain applied in this work ($e_f < 0.32$) did not increase the low initial orientation of lamellae normal to the LD. The lamellae
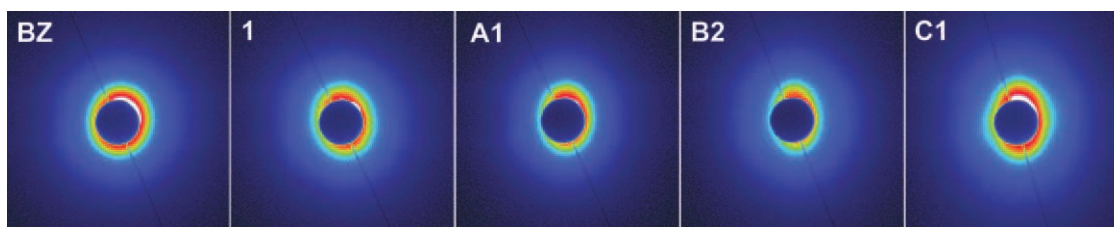
Figure 5 2-D SAXS patterns of selected Chirulen samples. The samples were illuminated along the radial (transverse) direction. The LD was vertical. Refer to Table I for the sample codes. [Color figure can be viewed in the online issue, which is available at wileyonlinelibrary.com.]

remained lightly oriented with their normals preferentially along the LD, even in sample C of the highest e_f (0.32). Such an observation was in line with previous reports and indicated that higher strains, well above $e_f = 0.6$, were needed to develop a strong lamellar orientation.[22,28] The long period estimated from the SAXS patterns was around 32–32.5 nm along the load direction and was slightly higher, approximately 32.5–33.5 nm, along the transverse (radial) direction. A slight correlation between the compression and long period was found in the deformed samples, with the long period measured along the LD tending to decrease a little with strain, whereas that measured along the transverse direction seemed to increase slightly. Both changes were primarily due to crystallographic slips active on plastic deformation.[22] There was practically no influence of irradiation on the long period.

Changes in the PE structure after plastic deformation and electron-beam irradiation

Figure 6 illustrates the evolution of selected structural parameters with plastic deformation and irradiation. Figure 6(a) shows that the plastic deformation alone resulted in a slight increase in the overall crystallinity (X_c) with increasing strain (however, the crystallinity determined from the DSC data was encumbered with a few percentage error of the method). Irradiation with electrons caused a further increase in the crystallinity in the entire range of the strain explored. These trends were confirmed by the FTIR data, which demonstrated that the sa values of the deformed samples A, B, and C (the parameter illustrated changes in the amount of parallel arranged chains in a modified sample relative to the initial raw sample BZ) showed a stable successive growth, which was rather small for samples that were only deformed and yet notably larger for samples crosslinked with electron beams after compression [cf. Fig. 6(b)]. On the other hand, deformation reduced hmf [cf. Fig. 6(c)]. This might suggest some fragmentation of the very long chains of UHMWPE upon plastic deformation, even at the low strains used in this work. Such behavior was plausible,

especially for the longest macromolecules, which were highly entangled and, moreover, frequently engaged in several adjacent lamellar crystals. Because of that, they were extremely constrained, and even the low overall strain led to a full extension of the constrained fragments of chains within the amorphous phase and led to high local stress concentrations; this, in turn, resulted in chain rupture. This could have partially removed some constraints and allowed for better spatial arrangement of the macromolecules. The irradiation with electron beams led to the crosslinking of the PE chains, which resulted in an increase in the insoluble fraction and a reduction in the low-molecular, soluble fraction in the irradiated samples. A combined application of deformation and crosslinking by irradiation showed their synergistic impact. This effect was emphasized by the achievement of significant increases in X_c and sa of the deformed samples after their irradiation.

Changes in the mechanical properties

H and E were evaluated from the data collected in the microindentation test. Samples were probed in this test by indentation in the direction parallel to the LD in the prior compression (i.e., the plane of the sample was perpendicular to LD). By analyzing the deformation-related changes in H and E, one can find small decreases in both H and E with increasing strain. This is illustrated in Figure 7. Such a behavior reflects a developing, although still quite low, orientation of the material with chains orienting preferentially away from the LD. Increases in H and E were observed in the irradiated samples, especially in those irradiated with a double dose (52 kGy), for which both H and E increased above the level of the initial raw material, all independently of the strain applied. Such a behavior was justified by an increase in the crystallinity and a simultaneous and significant increase in the degree of crosslinking in the amorphous phase after even a single irradiation dose and an even larger increase after the second dose. These made both the crystalline and amorphous phases stiffer.
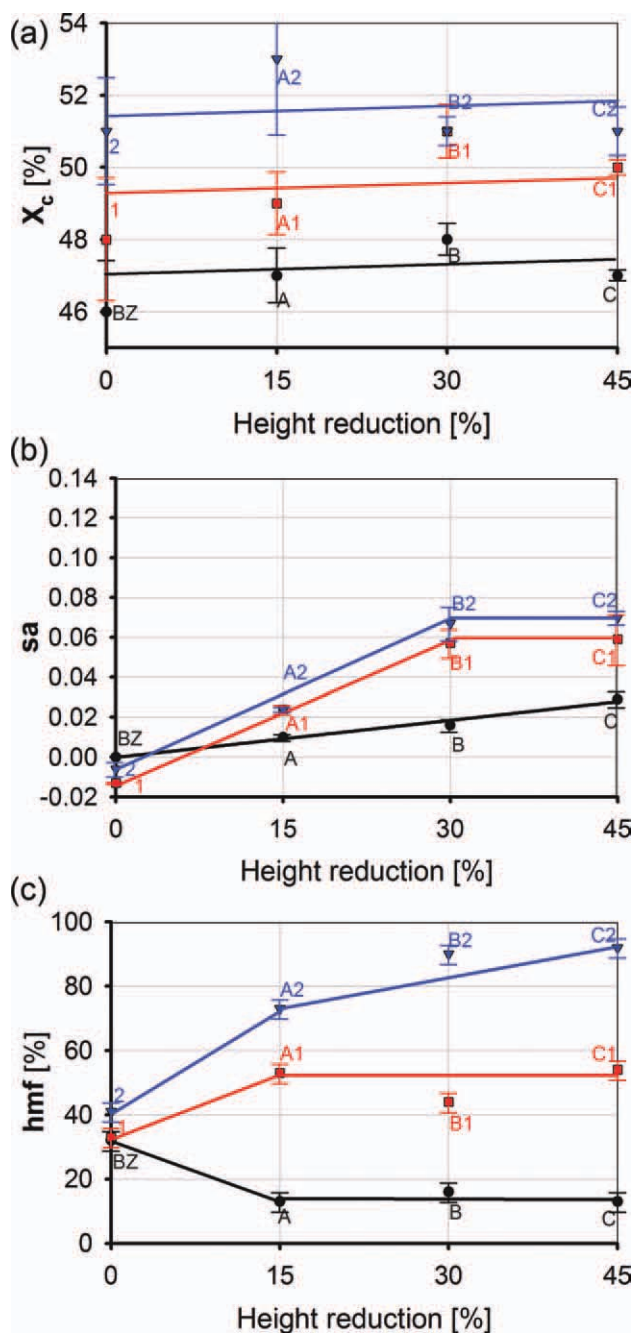
Figure 6 Effect of plastic deformation and subsequent irradiation with an electron beam on the (a) degree of crystallinity, (b) sa of the polymer, and (c) content of the insoluble, high-molecular fraction. Refer to Table I for the sample codes. [Color figure can be viewed in the online issue, which is available at wileyonlinelibrary.com.]

The plastic deformation of the base material BZ by uniaxial compression also caused an increase in the scratch susceptibility characterized by the depth of the scratch groove under load PD and its final depth after retraction of the tool and material recovery, RD, which increased monotonically with a reduction in the sample height, that is, with increasing strain, as illustrated in Figure 8. Similar to that in the

microindentation test, the plane tested in this experiment was perpendicular to the LD. The application of the second step of treatment, that is, electron-beam irradiation, resulted, in turn, in an improved scratch resistance of the material; the initial and the final scratch depths decreased with irradiation, independently of the strain (see Fig. 8).

Stereometric analysis of the scratch traces indicated that increasing the plastic deformation resulted in increases in A and B in the PE during scratch testing (A and B are defined in Fig. 1). An opposite effect was evoked by the irradiation of the samples with electron beams of 26- and 52-kGy doses: A and B decreased. The changes in A and B are presented in Figure 9(a,b), respectively. The proportion of A and B indicated that about one-third of the material from scratch groove A underwent permanent deformation and formed B. β was determined on the basis of the A and B values and, for the investigated set of samples, fell within the range 0.6–0.75. This indicated the presence of an extrusion micromechanism with a low ploughing component (for which β → 0). Lower values of β, decreasing with increasing
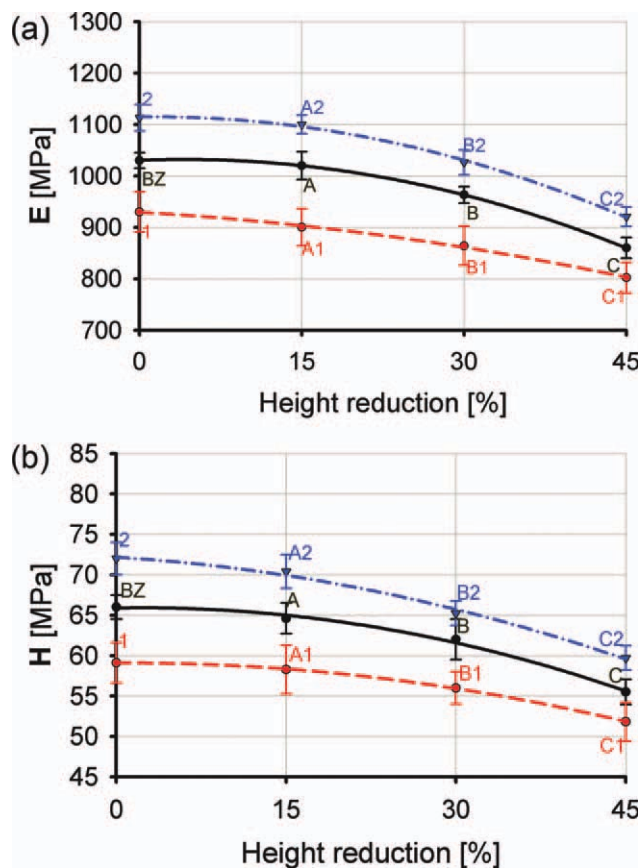

Figure 7 Influence of plastic deformation and subsequent irradiation with an electron beam on (a) E and (b) H. Refer to Table I for the sample codes. [Color figure can be viewed in the online issue, which is available at wileyonlinelibrary.com.]
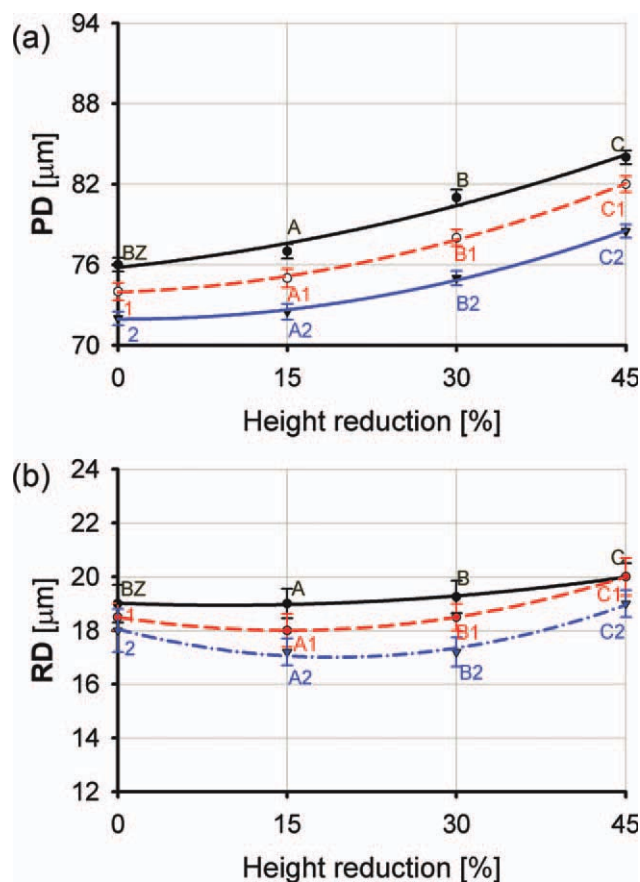
Figure 8 Influence of plastic deformation and subsequent irradiation with an electron beam on the susceptibility to scratching: (a) the depth of the scratch under load (PD) and (b) after unloading and strain recovery (RD). Refer to Table I for the sample codes. [Color figure can be viewed in the online issue, which is available at wileyonlinelibrary.com.]

strain, were characteristic of the samples that were only deformed and not irradiated after. This result confirmed their higher susceptibility to plastic deformation [cf. Fig. 9(c)]. This susceptibility decreased as the samples were posttreated by the irradiation.

Analyses of the results of the micromechanical studies presented in Figure 7–9 indicated that the most advantageous properties were found in samples A1 and A2 and B1 and B2, which were compressed by height reductions of 15 and 30%, respectively, and subsequently irradiated with a single or double electron-beam dose (26 or 52 kGy, respectively).

Changes in the tribological wear after the modification of PE

To verify the conclusions of the previous section, we subjected the investigated UHMWPE samples to interaction in a friction kinematical couple with a counterpartner made of a cobalt–chromium alloy (Vitalium, Faculty of Materials Engineering and Metallurgy, Silesian University of Technology, Katowice,

Poland). This system roughly approximated the working conditions of a joint endoprosthesis. The polymer specimen was oriented with the normal of the friction plane perpendicular to the to LD of the compressed sample (see Fig. 1). The unidirectional sliding direction within the friction plane was normal to the LD. After the test, the mass decrement (Z_m) and the linear dimension in the direction normal to the friction plane (thickness of the sample)
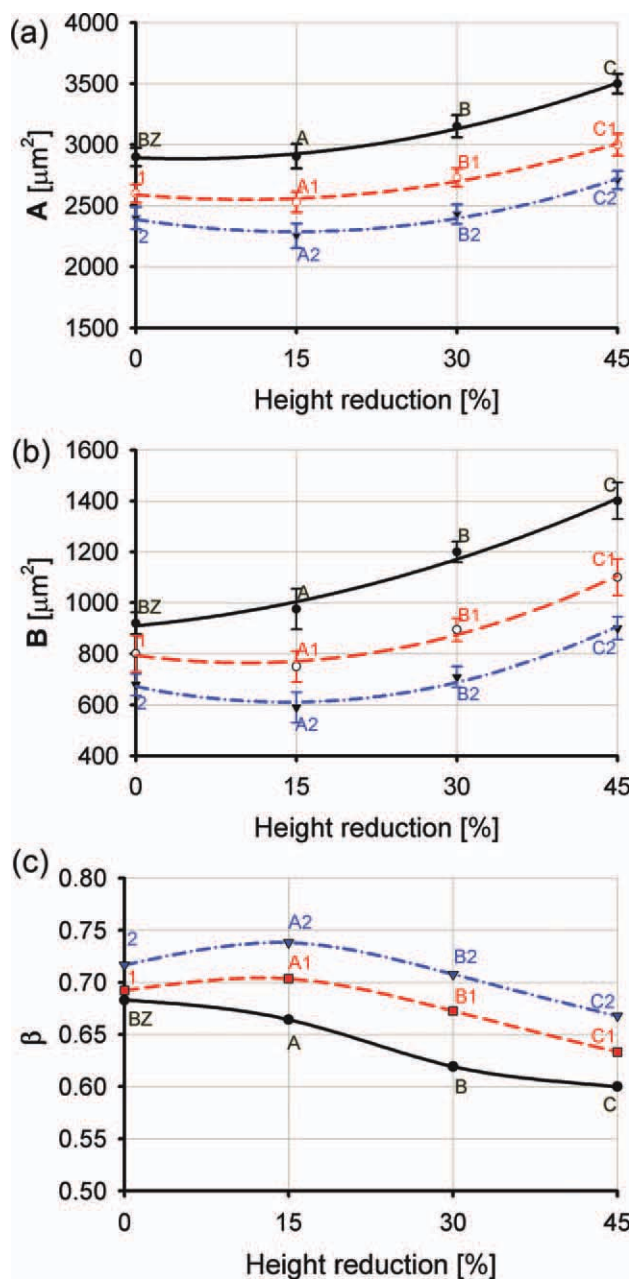

Figure 9 Influence of plastic deformation and subsequent irradiation with an electron beam on the susceptibility to scratching: (a) A and (b) B formed during a scratch test. β was calculated from the scratch profile data. Refer to Figure 1 for an explanation of A and B and to Table I for the sample codes. [Color figure can be viewed in the online issue, which is available at wileyonlinelibrary.com.]
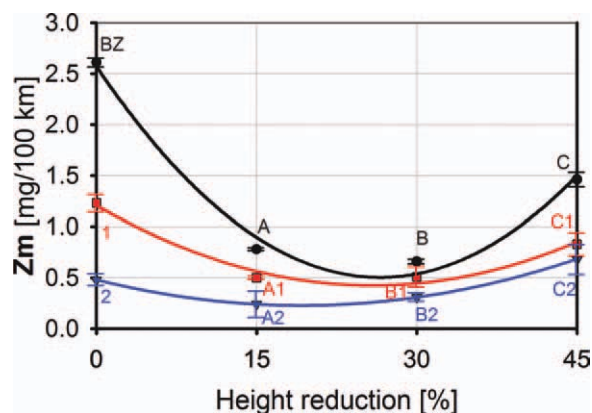
Figure 10 Dependence of the tribological wear (Z_m) on the plastic deformation and irradiation. Sample codes according to Table I. [Color figure can be viewed in the online issue, which is available at wileyonlinelibrary.com.]

were measured. A graphical presentation of the results of PE wear in such a tribological test is given in Figure 10.

Analysis of the results showed that the lowest wear [weight loss (Z_m)] occurred in the deformed and irradiated samples A1 and A2 and, especially, B1 and B2, with strains (e_f) of 0.14 and 0.21, respectively. This result confirmed the conclusions from

the previous section. The wear of these samples was approximately five times lower than that of the sample of the raw polymer BZ and about two times lower than those of the samples that were irradiated without prior deformation (samples 1 and 2). Such a significant improvement in the functional properties was apparently a result of the polymer structure, which was altered through the applied deformation–irradiation procedure. In these four most advantageous cases, the material was oriented only slightly, and this orientation was stabilized by the crosslinking produced by irradiation, whereas the semicrystalline morphology of the initial PE and a balanced proportion of high- and low-molecular fractions were preserved (cf. Fig. 6). Note that samples C, C1, and C2, with the highest deformation studied ($e_f = 0.32$), again exhibited a larger wear. The structures of samples of the A and B series contributed to reduction in the plastic deformation and wear of the polymer upper layer during the wear test with a metal–polymer couple.

Microscopic observation with the scanning electron microscope of the near-surface layer after the wear test (the most upper layer was removed by permanganic etching) revealed that lamellae within this layer underwent some reorientation because of sliding friction interaction. Example micrographs are
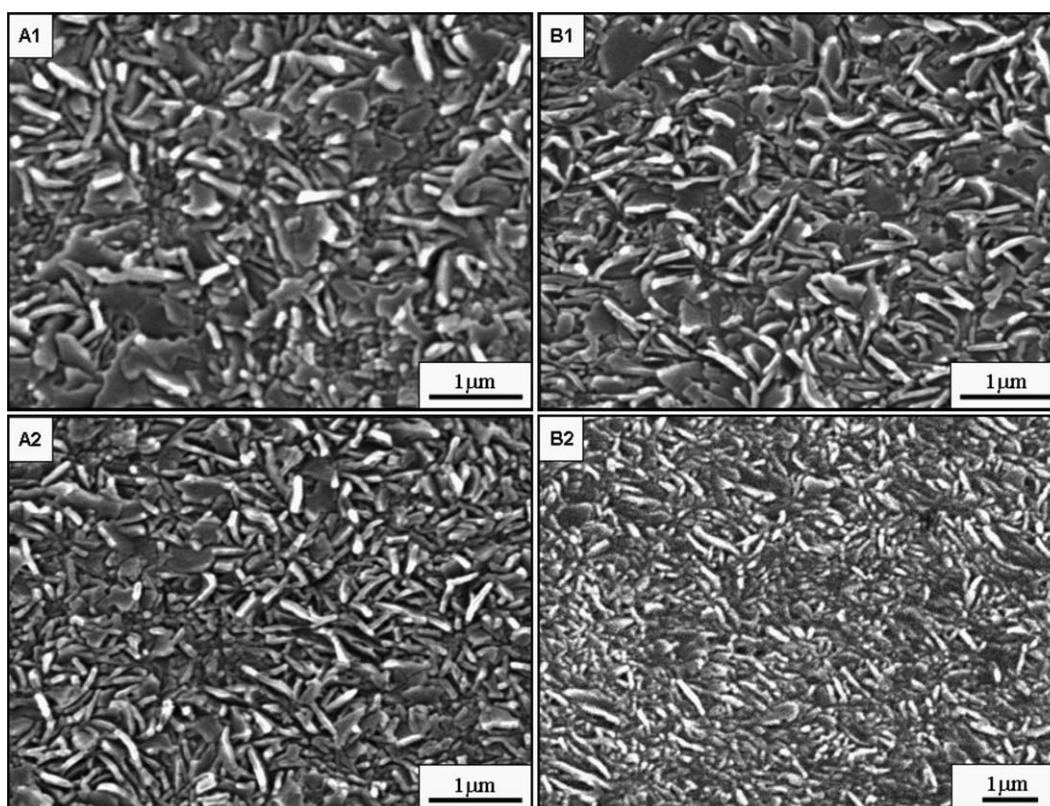

Figure 11 Scanning electron micrographs of the near-surface layers of the UHMWPE samples after the tribological wear test. The observation plane, parallel to the friction plane and located a few micrometers beneath the friction plane, was exposed by permanganic etching. The direction of friction was vertical. Refer to Table I for the sample codes.

presented in Figure 11. In the samples not deformed before the tribological experiment, the dominating lamellar orientation within the near-surface layer after tribological testing was the flat-on orientation. This orientation was apparently induced by a long, unidirectional sliding motion. In the case of the pre-oriented samples, we observed, however, in the near-surface layer a noticeable fraction of edge-on oriented lamellae. The fraction of edge-on orientation increased with increasing strain and with increasing crosslinking degree (dependent the irradiation dose) for a given strain. This was probably a result of some lamellae orientation on compression, in which the orientation was additionally fixed and stabilized to some extent by the crosslinking of amorphous interlamellar layers produced by irradiation. It seemed obvious that an increase in the amount of lamellae oriented edge-on contributed to the reduction in the wear in the tribological test. The presented mixed structure orientation (with a flat-on and edgewise arrangement of lamellae in relation to the interacting surface) in the upper layer of the deformed and irradiated samples A1, B1, A2, and B2, with an improved resistance to plastic deformation during the wear test created appropriate conditions for reducing the wear of UHMWPE and led to an improvement in its functional properties.

CONCLUSIONS

The results reported in this article demonstrate that the plastic deformation of PE by uniaxial compression, conducted in the low-strain region, distant from the stress hardening area with a considerable orientation of polymer chains, fulfilled its role of a material structure-modification initiator. This structure adjustment was significantly supported by polymer crosslinking, in response to the irradiation of the deformed material. The contribution of the high-molecular fraction, crystallinity, and sa of the polymer chains increased. The crosslinking within the amorphous layers stabilized to some extent the orientation of lamellae produced by deformation, which together decreased the susceptibility of such a modified material to permanent plastic deformation.

The PE structure achieved by physical modification brought about an enhancement of the micromechanical properties determined by means of microindentation and sclerometry. Although the polymer resistance to scratching increased, its susceptibility to plastic deformation and the component of the ploughing wear micromechanism decreased. After irradiation with the 52-kGy dose, hardness and Young's modulus (E) increased as well. It is also important that during operation of the PE–metal kinematical couple, some reorientation of the lamellar structure occurred in an upper near-surface layer of

the polymer, partly because of its local plastic deformation, which accompanied the operation of the kinematic couple. Depending on the strain produced by the prior compression and the contribution of the high-molecular, crosslinked fraction, the operation of the kinematical sliding couple led to the formation of, in the PE upper layer, a structure with a higher or lower fraction of flat-on and edge-on oriented lamellae in relation to the polymer working surface. It appeared that contents of 70–80% of the insoluble fraction sufficiently limited the thickness of the plastically deformed upper layer and ensured proper dominance of the edgewise orientation of lamellae in relation to the friction surface. In such cases, a large (nearly fivefold) reduction in PE wear was observed during the 100-h tribological tests in comparison with the input unmodified material. This result indicates the possibility of significant improvement in the operational durability of the polymer–metal system by appropriate physical modification of the polymer. The UHMWPE grade used in this work was Chirulen 1120. It would seem useful to verify the presented results for GUR 1020 and GUR 1050 UHMWPE grades, with higher molecular weights than that of PE tested here, as these materials are nowadays applied widely in alloplasty procedures.

References

1. Pruski, K.; Górecki, A.; Jabłoński, T. Ortopedia Traumatologia Rehabilitacja 2001, 3, 15.
2. Greer, K. W.; Hamilton, J. V.; Cheal, E. J. In Encyclopedic Handbook of Biomaterials and Bioengineering: Part B: Applications; Wise, D. L., Ed.; Marcel Dekker: New York, 1995; p 613.
3. Edidin, A. A.; Rimnac, C. M.; Kurtz, S. M. Wear 2001, 250, 152.
4. Hip Replacement: Current Trends and Controversies; Sinha, R., Ed.; Marcel Dekker: New York, 2002.
5. Kurtz, S. M.; Muratoglu, O. K.; Evans, M.; Edidin, A. A. Biomaterials 1999, 20, 1659.
6. Muratoglu, O. K.; Cook, J. L.; Jasty, M.; Harris, W. H. Presented at the 44th Annual Meeting of the Orthopaedic Research Society, New Orleans, LA, March 1998.
7. Premnath, V.; Harris, W. H.; Jasty, M.; Merrill, E. W. Biomaterials 1996, 17, 1741.
8. Streicher, R. M. Radiat Phys Chem 1995, 46, 893.
9. Bell, C. J.; Walker, P. S.; Abeysundera, M. R.; Simmons, J. M.; King, P. M, Blunn, G. W.; J. Arthroplasty 1998, 13, 280.
10. Kurtz, S. M.; Mazzucco, D.; Rimnac, C. M.; Schroeder, D. Biomaterials 2006, 27, 24.
11. Ohta, M.; Hyon, S.-H.; Tsutumi, S. Wear 2003, 255, 1045.
12. Marrs, H.; Barton, D. C.; Doyle, C.; Jones, R. A.; Lewis, E. L. V.; Ward, I. M.; Fisher, J. J Mater Sci Mater Med 2001, 12, 621.
13. Addiego, F.; Buchheit, O.; Ruch, D.; Ahzi, S.; Dahoun, A. Clin Orthopaedics Rel Res 2011, 469, 2318.
14. Li, D. S.; Garmestani, H.; Ahzi, S.; Khaleel, M.; Ruch, D. J Eng Mater Technol 2009, 131, 0412111.
15. Maszybrocka, J.; Cybo, J.; Cwajna, J. Mater Charact 2009, 60, 1139.
16. Cybo, J.; Maszybrocka, J.; Frąckowiak, J. E.; Inżynieria Mater 2004, 3, 295.
17. Maszybrocka, J.; Cybo, J.; Frąckowiak, J Mater Sci Forum 2006, 513, 75.

18. Cybo, J.; Maszybrocka, J.; Cwajna, J. Mater Charact 2006, 56, 363.
19. Maszybrocka, J.; Cybo, J.; Cwajna, J. Mater Charact 2009, 60, 1139.
20. Kurtz, S. M.; Villarraga, M. L.; Herr, M. P.; Bergstrom, J. S.; Rimnac, C. M.; Edidin, A. A. Biomaterials 2003, 23, 3681.
21. Bartczak, Z.; Kozanecki, M. Polymer 2005, 46, 8210.
22. Bartczak, Z.; Lezak, E. Polymer 2005, 46, 6050.
23. Wunderlich, B.; Czornyj, G. Macromolecules 1977, 10, 906.
24. Czaja, K.; Sudol, M. Radiat Phys Chem 2011, 80, 514.

25. The UHMWPE Handbook: Ultra High Molecular Weight Polyethylene in Total Joint Replacement; Kurtz, S. M., Ed.; Academic: San Diego, 2004.
26. Olley, R. H.; Hodge, A. M.; Bassett, D. C. J Polym Sci Polym Phys Ed 1979, 17, 627.
27. Bartczak, Z.; Argon, A. S.; Cohen, R. E. Macromolecules 1992, 25, 5036.
28. Boontongkong, Y.; Cohen, R. E.; Spector, M.; Bellare, A. Polymer 1998, 39, 6391.